

*Electronic Supplementary Information*

DNA-nanoparticle actuator enabling optical  
monitoring of nanoscale movements induced by  
electric field

*Kosti Tapio<sup>1</sup>, Dongkai Shao<sup>1‡</sup>, Sanna Auer<sup>2‡</sup>, Jussipekka Tuppurainen<sup>3</sup>, Markus Ahlskog<sup>1</sup>, Vesa  
P. Hytönen<sup>2</sup>, J. Jussi Toppari<sup>1\*</sup>*

<sup>1</sup>Department of Physics and Nanoscience Center, P.O. Box 35, FI-40014  
University of Jyväskylä, Finland.

<sup>2</sup>Faculty of Medicine and Life Sciences and BioMediTech, University of Tampere, Arvo Ylpön  
katu 34, FI-33520 Tampere, Finland and Fimlab laboratories, Biokatu 4, FI-33520 Tampere.

<sup>3</sup>BioNavis Ltd, Hermiankatu 6-8 H, FI-33720 Tampere, Finland

Email: [j.jussi.toppari@jyu.fi](mailto:j.jussi.toppari@jyu.fi)

KEYWORDS Gold nanoparticle, DNA, avidin, biotin, surface plasmon, actuator, electric field.

## Note 1 - UV-vis spectra and particle concentrations

The UV-vis samples are prepared by mixing 10  $\mu\text{l}$  of the biotin-AuNPs or the control sample to 1 ml of ddH<sub>2</sub>O in 1.5 ml disposable UV-cuvettes (Brand GMBH). The cuvette was placed inside Perkin Elmer Lambda 850 UV-vis spectrometer and the UV-vis absorption spectra were measured from 350 nm to 800 nm (Figure S1). The concentrations of the AuNP samples were calculated from the UV-vis absorption spectra using the Beer-Lambert law<sup>1</sup> (Table S1). The LSPR peak maxima in Figure S1 were between 554 nm and 560 nm, which indicate that the plasmonic properties have not significantly altered from the original, plain particle, and we used the manufacturer provided molar extinction coefficient<sup>2</sup> in all of the concentration calculations.

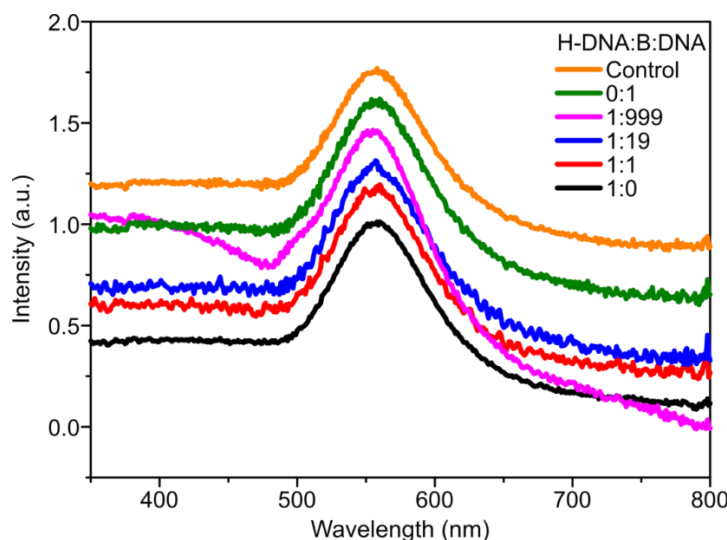


**Figure S1.** The UV-vis absorption data of different hairpin-DNA (H-DNA) coated AuNP samples used in the study.

**Table S1:** Concentrations of the different biotin-AuNP samples

AuNP sample	$N_{\text{hairpin-DNA}} : N_{\text{blocking-DNA}}$	Concentration (pM)
hairpin-DNA	1:999	127
hairpin-DNA (plain)	1:0	223
DNA-s15nm	1:999	130
DNA-s8nm	1:999	77
DNA-s3nm	1:999	78
Control AuNP	-	122

<sup>1</sup> IUPAC. Compendium of Chemical Terminology, 2nd ed. (the "Gold Book"). Compiled by A.D. McNaught and A. Wilkinson. Blackwell Scientific Publications, Oxford (1997).

<sup>2</sup> <http://www.sigmaaldrich.com/technical-documents/articles/materials-science/nanomaterials/gold-nanoparticles.html>

## Note 2 - DLS characterization of the hydrodynamic diameter of the hairpin-DNA samples

The hydrodynamic diameter of the hairpin-DNA functionalized AuNPs and the control sample were recorded using BECKMAN Coulter N5 submicron Particle size Analyzer. First, the 4 ml cuvette was washed three times with ddH<sub>2</sub>O that was filtered using 0.1 μm pore size syringe filter. Then, 10 μl of the sample was mixed well with 4 ml of ddH<sub>2</sub>O, any bubbles on the cuvette walls were pumped away and the cuvette was placed inside the analyzer. The sample was thermally stabilized for 5 min, and after that the average hydrodynamic diameter was recorded for 5 runs, and each run lasted 120 s. Figure S2 shows the average hydrodynamic diameters of the hairpin-DNA samples as a function of the hairpin-DNA and blocking-DNA ratio.

The hydrodynamic diameter decreases overall, when the amount of hairpin-DNA decreases, since the blocking-DNA is much shorter than the hairpin-DNA, which is well seen in fig. S2 below. However, due to large variations in the result with lower amount of hairpin-DNA, we can only qualitatively correlate the hydrodynamic diameter to the amount of biotin groups on the surface of biotin-AuNPs by this method.

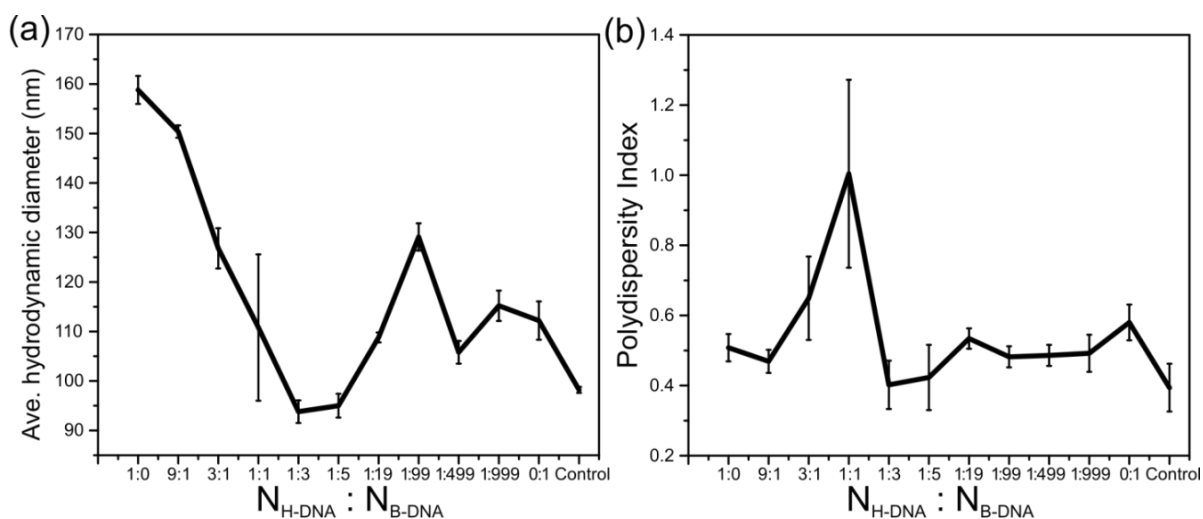


**Figure S2.** The average hydrodynamic diameter and the corresponding polydispersity index of the different hairpin-DNA-AuNPs after fabrication. (a) The average hydrodynamic diameter of the hairpin-DNA functionalized AuNP samples in respect to the hairpin-DNA to blocking-DNA ratio. The hydrodynamic diameter decreases overall, when the amount of hairpin-DNA decreases, since the blocking-DNA is much shorter than the hairpin-DNA. (b) The polydispersity index for the same samples. The hairpin-DNA-AuNP samples have roughly similar polydispersity index as the control sample, which indicates that the AuNPs are not aggregating due the DNA or salt buffer.

### Note 3 - Zeta potential characterization of the biotin-AuNP samples

Zeta potentials of different DNA coated AuNP samples were measured using Zetasizer Nano ZS (Malvern Instruments, Worcestershire, UK). Typical experiment was carried out by diluting the sample 400 $\times$  using NaPo-NaCl buffer in disposable folded capillary cells (count rate 20-107 kcps) and measuring the zeta potential at 20 $^{\circ}$ C for 60 s. The different zeta potential curves for the 0.1 % hairpin-DNA-AuNP, 3 nm DNA linker, 8 nm DNA linker and 15 nm DNA linker samples are shown in Figure S3a-d. The percentages of negative and positive particles in Figures S3a-d were solved by calculating the areas of negative side and positive side of the curves and dividing these areas by the corresponding total area (see Table S2). The hairpin-DNA sample and the DNA-s8nm have both one positive peak and one negative main peak, whereas the DNA-s3nm and DNA-s15nm samples only one negative main peak (see Table S2).

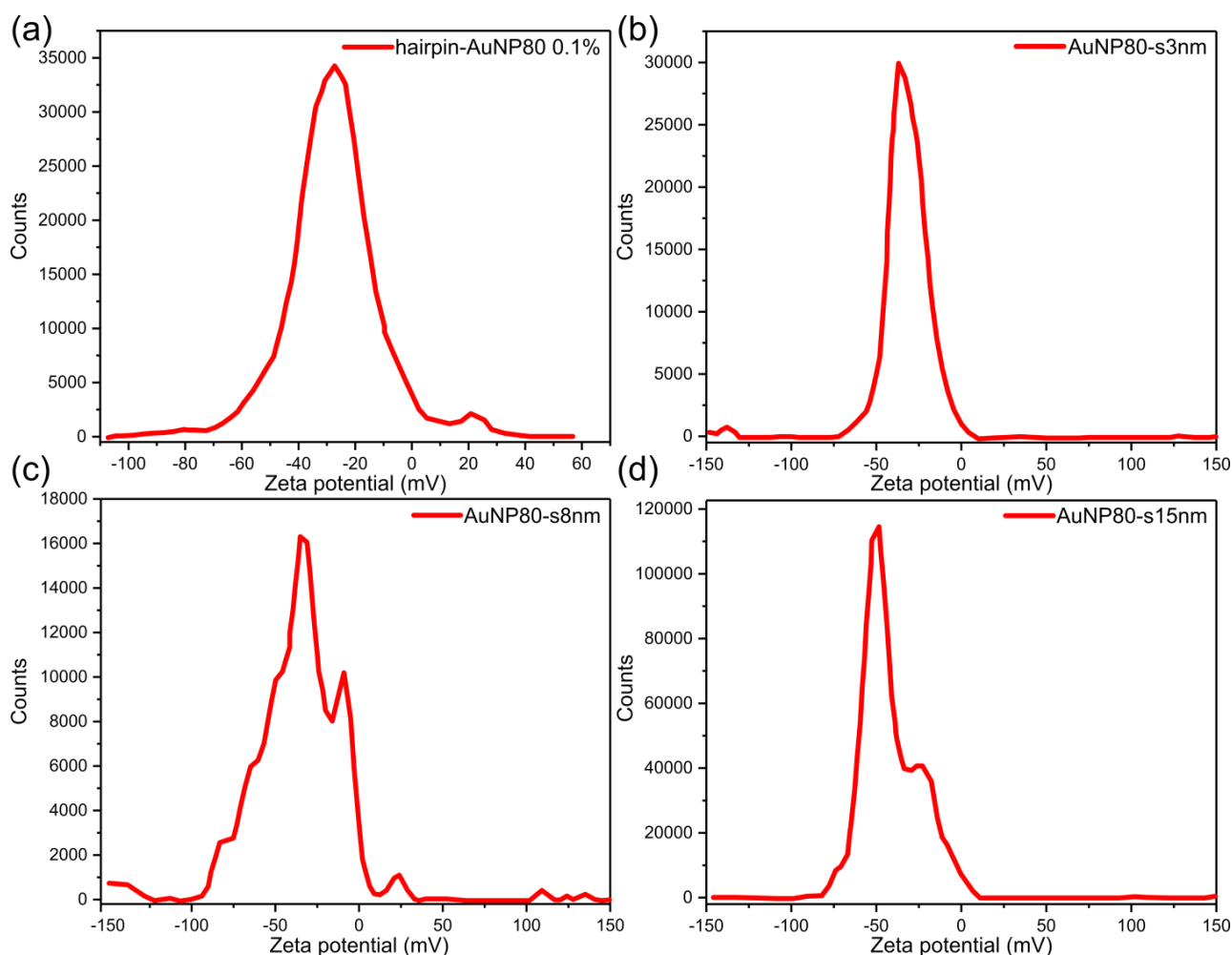


**Figure S3.** Zeta potential distribution of (a) the 0.1 % hairpin-DNA-AuNP (0.1%) and (b) 3 nm, (c) 8 nm and (d) 15 nm ssDNA linker coated AuNPs.

**Table S2:** The charge composition of the biotin-AuNP samples

Sample	Neg. Peak (mV)	Pos. Peak (mV)	Neg. particles (%)	Pos. particles (%)
hairpin-DNA	-27.3	+20.8	94.2	5.8
DNA-s15nm	-48.6	–	99.1	0.9
DNA-s8nm	-35.1	24.0	96.5	3.5
DNA-s3nm	-36.9	–	98.7	1.3

#### Note 4 - Additional SPR biosensor data

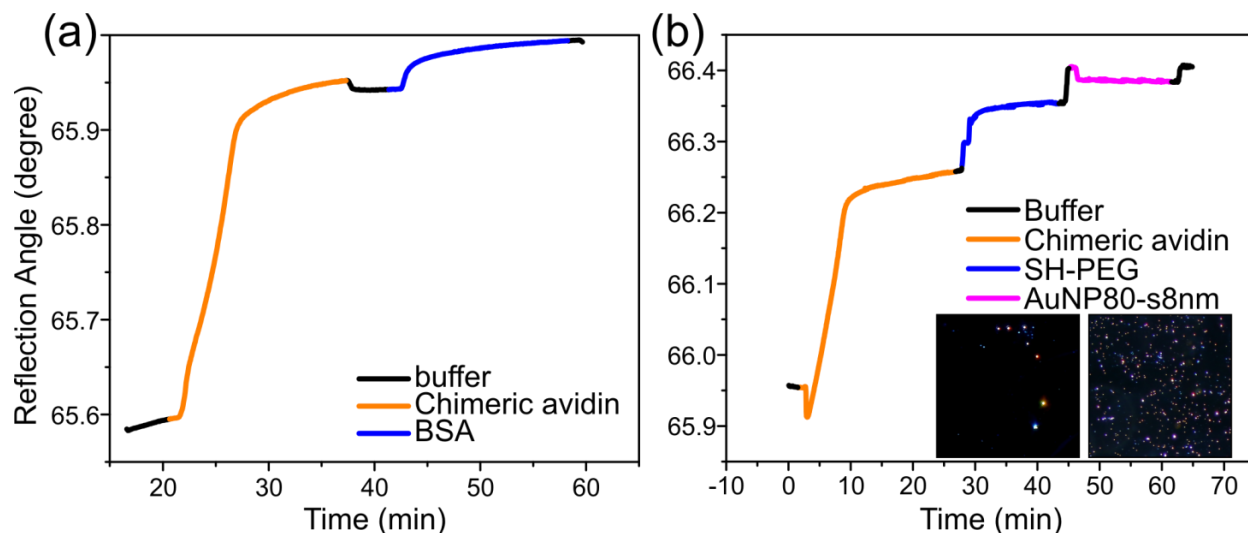


**Figure S3.** RA-SPR characterization of chimeric avidin, BSA and SH-PEG layer formation on gold surface and AuNP-s8nm binding to the chimeric avidin. The different colors represent the injection phase of the corresponding material in the curves. (a) The SPR characterization of the different assembly steps for chimeric avidin and BSA immobilization in Figures (1a) and (1b). The binding of chimeric avidin, blocking agent (BSA) was detected as a positive shift in the resonant angle. (b) The SPR characterization of the assembly steps for chimeric avidin, SH-PEG and 8 nm linker DNA coated AuNP immobilization. The binding of chimeric avidin, blocking agent (SH-PEG) is detected as a positive shift in the resonant angle but, for the 8 nm linker DNA coated AuNPs, the overall shift is negligible due to the plasmonic coupling between the surface and the AuNPs. The dark field images of the arbitrary, plain gold surface (left inset) and the channel after the AuNP deposition (right inset) show still that the AuNPs are binding to the surface.

## Note 4 – Calculating the layer composition chimeric avidin for 0.1% biotinylated hairpin-DNA sample in the DLS measurements

In this section, the chimeric avidin layer composition of 0.1% hairpin-DNA sample is evaluated based on the DLS measurements. The control sample without any DNA showed 20% increase in the hydrodynamic diameter  $D$ , which can be due to non-specific binding of avidin on AuNP or bulk effects. The 0.1% hairpin-DNA sample had 30% increase in the hydrodynamic diameter. To estimate the avidin coverage, i.e., number of avidin layer on the 0.1% hairpin-DNA sample, we assume that during the aggregation process, there are no dimers forming and the increase in  $D$  is due to both the bulk effects, as in the case of the control sample, and the avidin binding to the surface of hairpin-DNA-AuNPs. Then the hydrodynamic diameter of after the aggregation process is

$$D_{final} = D_{AuNP} + D_{avidin} = 80 \text{ nm} + 5 \text{ nm} \cdot 2n,$$

where  $n$  is the number of avidin layers and the factor 2 is due to the fact that one needs to count twice the avidin layer when considering the diameter of the avidin coated AuNPs. Then  $n$  can be solved by assuming, that since the control sample had 20% increase in the  $D_{rel}$ , we can subtract this from the  $D_{rel}$  of the 0.1% hairpin-DNA sample:

$$\begin{aligned} D_{rel} &= \frac{D_{final} - D_{ini}}{D_{ini}} = 0.3 - 0.2 = 0.1 \\ \frac{D_{final}}{D_{ini}} &= \frac{2n \cdot 5 \text{ nm} + 80 \text{ nm}}{80 \text{ nm}} = 1.1 \\ \frac{2n \cdot 5 \text{ nm}}{80 \text{ nm}} &= 0.1 \Rightarrow n = 0.8 \approx 1 \end{aligned}$$

## **Note 5 - The sample holder and the single particle spectroscopy setup**

Figure S4 shows the sample holder and different assembly stages of the final measurement configuration. First, the fresh aluminum contacts were fabricated to make contact for the gold coated silicon chip (Figures S4a-c) using aluminum tape. Next, the gold coated silicon chip was glued to the aluminum contact using a silver paste and varnish (Figure S4c). The silver paste was only added to the backside gold contacts and the silver paste was circled using the varnish. The TCEP-treated chimeric avidin solution was added to the surface and the avidin was incubated for 30 min (Figure S4d). The surface was washed with PBS and the process was repeated for BSA, except the washing was done using 0.1 mM NaPhos and 1 mM NaCl buffer (pH 7.6). After washing the BSA away, the surface was kept under humid conditions and ITO cover glass was fixed on top of the surface using scotch tape (Figure S4e). Next, the fluid channels were pre-wetted using the same NaPhos and NaCl buffer (Figure S4f), the holder placed in the microscope setup and the pump was connected to the output fluid channel. The AuNP deposition was carried out by injecting 50 - 100  $\mu$ l of 10 $\times$ diluted AuNP solution (see Table 1 for the concentration) to the input channel, waiting for 15 to 90 min until enough particles were immobilized, turning the pump on and flushing the chamber by injection the same NaPhos and NaCl buffer to the input channel and pumping the excess liquid from the output channel (Figure S4g). Figure S4h shows image of the holder with a gold coated silicon chip after measurement.

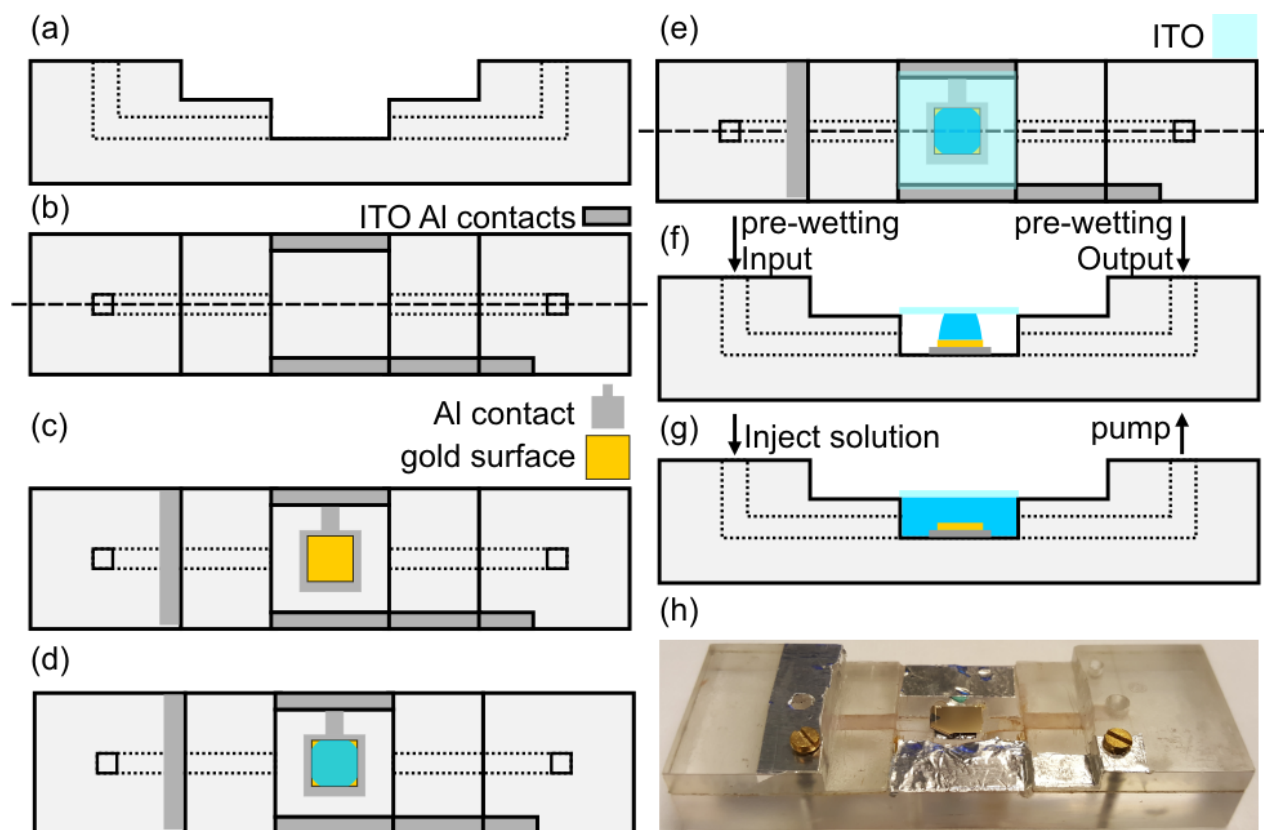


**Figure S5.** An image of the sample holder and different assembly stages before and during the AuNP deposition. (a) Initial schematic side view of the holder without the aluminum contacts for the silicon chip. Dotted lines indicates the fluid channels. (b) A schematic top view of the holder without aluminum contact, where the dashed line indicates the cross section in (a). (c) In the first step, aluminum contacts were fabricated and the gold coated silicon was clued to the contacts using varnish and silver paste. (d) Chimeric avidin and BSA solution were incubated for 30 min, followed by washing step. (e) Next, the avidin and BSA coated gold surface was sealed into chamber using the ITO cover glass. The cross section of (f) is indicated by the dashed line. (f) A schematic side view of the holder configuration in image (e). The fluid channels are pre-wetted before the AuNP deposition. (f) During the deposition, the AuNP solution was injected to the chamber and let incubate for 15 - 90 min. Then pump was turned on and NaPhos and NaCl buffer was added while pumping the excess liquid away. (h) Image of the sample holder without the ITO cover glass. The length of the holder is 75 mm and the width is 26 mm.

The single particle spectra were measured using Olympus BX51TRF microscope with Olympus MPLANFL N-objectives (5x / 20x / 50x) equipped with Princeton Instruments SP2150 (Acton) spectrograph and Andor Ivac DR-324B-FI spectroscopy CCD camera as shown in Figure S5a. The excitation light was generated using Olympus 75 W Xenon lamp (L2194-01) inside Olympus U-LH75XEAP0-1-6 lamp housing. Dark field imaging was carried out using Olympus DF U-MDF3 dark field cube. The light was collected to Thorlabs UM22-300-custom fiber (core size 300  $\mu\text{m}$ ) located in the output port of the microscope. The tip of the fiber was placed in the image plane of the port. The other end of the fiber was connected to a Thorlabs collimator that was in turn connected to a custom-made switch box (Thorlabs). The collimated

light was focused to slit of the spectrograph equipped with the CCD camera used to measure the spectra. The dark field optical images were acquired using a Canon EO5 6D camera. To reduce the background lighting, the whole setup was placed inside a shielded room, and to preserve optical and electrical isolation, Black box IC404A fiber extender was used to communicate between the microscope setup and the measurements computer. Mascot electronics CPD1502 power source was used to generate DC bias voltage and Fluke 111 multimeter was used to measure the DC voltage. Thorlabs M530L3 mounted LED was used to illuminate and highlight the position of the fiber on the sample. Figure S5b shows typical view of the gold surface after AuNP deposition, where the green dot is the image of the fiber tip. A xyz-micrometer translational stage was utilized to move the fiber in the microscope view. The spectra were recorded using Andor Solis (version 4.18) software and Canon EOS utility software was used to remotely operate the camera. The combined height of the of the liquid layer and the thickness of the ITO glass was designed to be less than 1 mm, since the focus length of the highest magnification object (50x) was 1 mm.

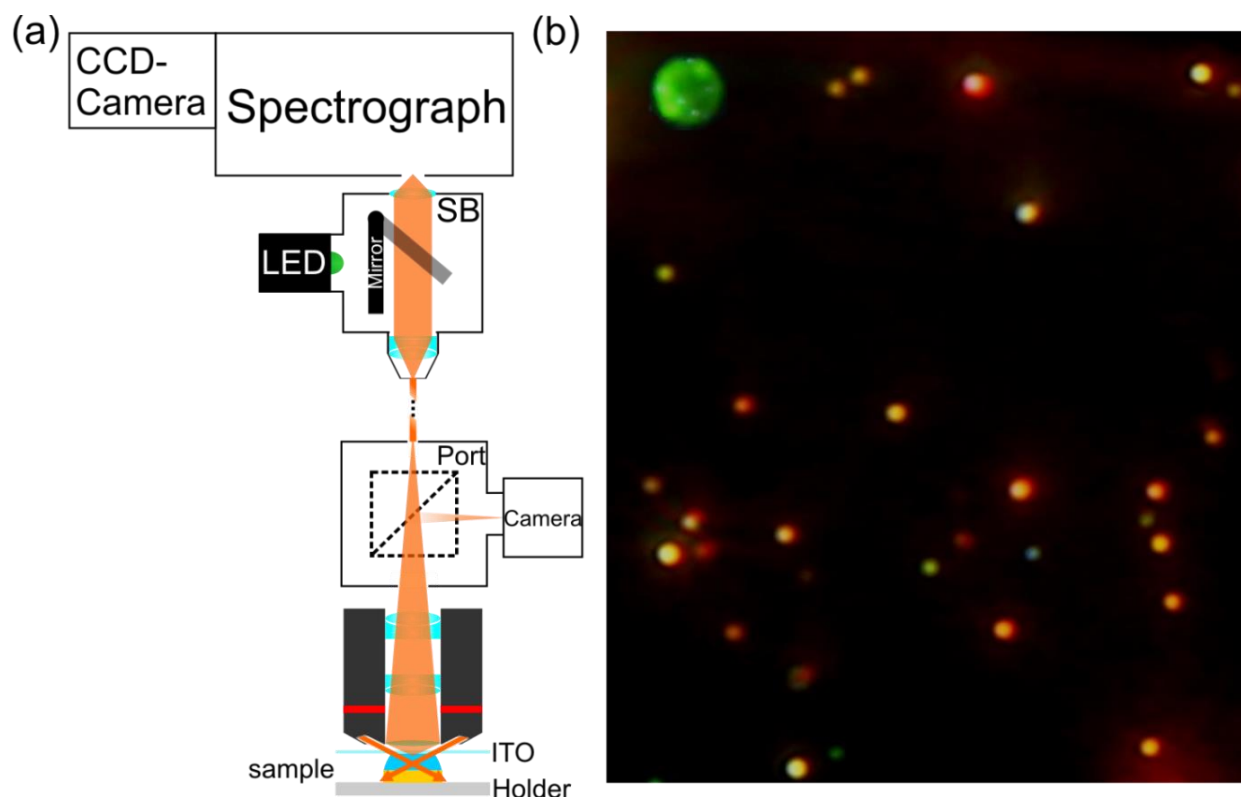


**Figure S6.** (a) A Schematic view of the microscope setup used in the nanoparticle analysis. (b) Typical dark field view of the gold surface after AuNP deposition, where the green dot in the upper left corner indicates the position of the illuminated fiber tip. The size of the image is roughly  $80 \mu\text{m} \times 95 \mu\text{m}$ .

## **Note 6 - Dark field images and calculating RGB values for AuNP samples**

During the voltage sweeping measurements, after each voltage change step an optical image of the surface-bound AuNPs was taken. The images were post-processed by slightly adjusting the brightness and the contrast to remove the background. Next, ImageJ-software was utilized to select the particles for RGB analysis by creating Region-Of-Interest (ROI) maps, where circular areas were drawn around the particles and each area or particle was assigned a number. The surface defects were left out of the ROI maps. These maps were defined for each sample separately, and we traced the RGB values of each particle from the first image to the last image (image = voltage step) using the ROI maps and the corresponding numbering. We converted the RGB data to the HSV data using the equations in the calibration section. For particle motion analysis, we initially selected particles, which changed the H value equal or more than  $40^\circ$ , when voltage was changed several times from positive to negative polarization or vice versa, since this is the smallest change from red (close to surface) to green-yellow (far away from surface) as shown in Figure S9. Then particle by particle, we analyzed the Hue behavior under electric field, and divided the particles into four groups: the Hue value changes as a step function to either high hue values ( $>100^\circ$ , group 3) or low Hue values ( $\approx 0^\circ$ , group 4) or the Hue value followed negative voltage (group 1) or positive voltage (group 2). Figures S7 and S8 show typical images of the analyzed samples, where color changing particles are circled. Notably, most of the particles didn't change color during the measurements. Each group was then plotted in separate histograms for each voltage value and for each sample.

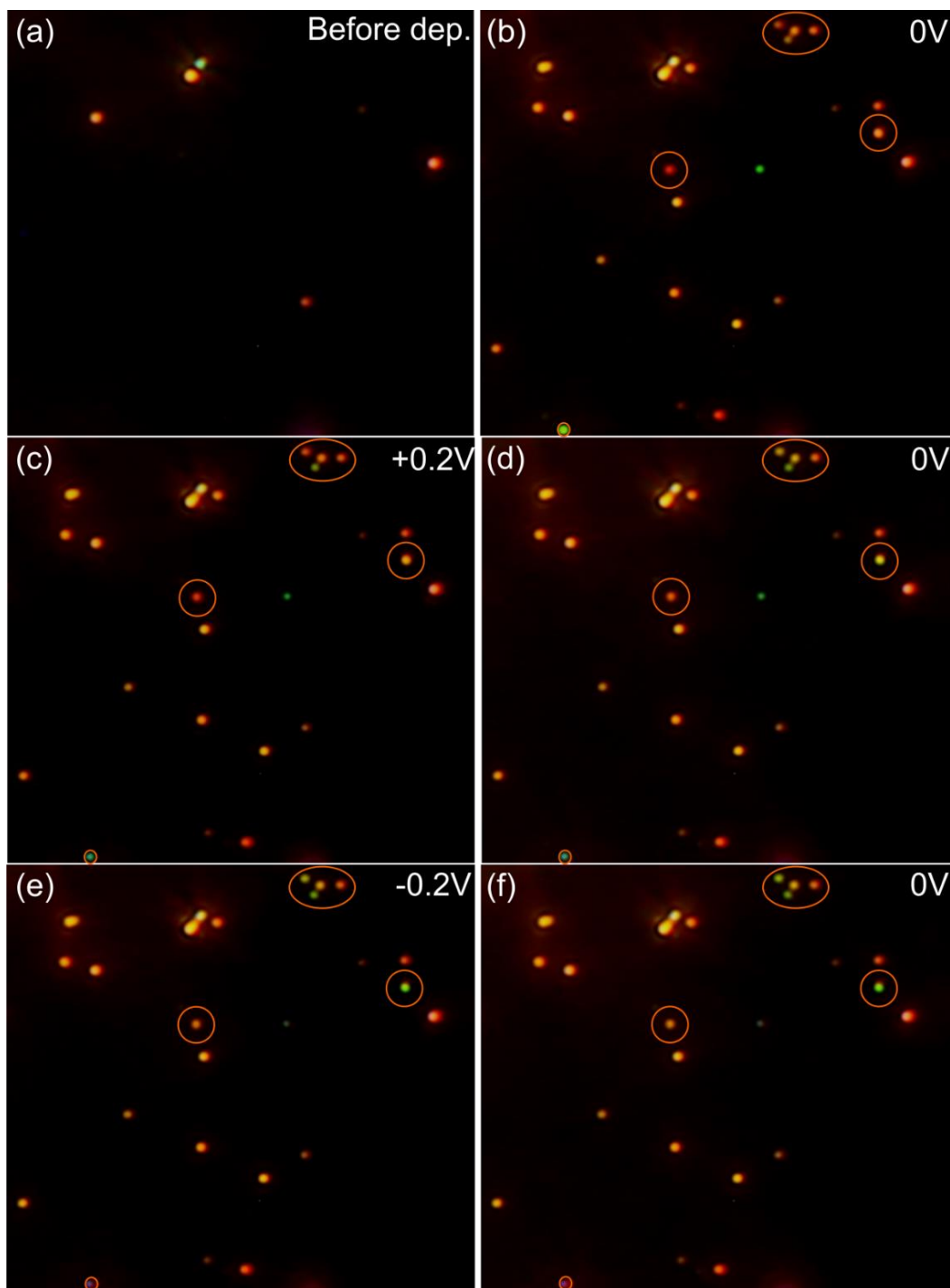


**Figure S7.** Dark field images of 0.1 % hairpin-DNA-AuNP sample before deposition and when the bias voltage was swept from 0 V to +0.2 V, then to -0.2 V and then back to 0 V. The AuNPs that change their color significantly during the measurements are circled. (a) The gold surface before AuNPs deposition. The objects seen in the image are surface defects. (b) The gold surface after AuNPs deposition and at zero biasing voltage. (c) The gold surface bound AuNPs under influence of +0.2 V bias voltage. (d) The gold surface bound AuNPs under influence of 0 V bias voltage. (e) The gold surface bound AuNPs under influence of -0.2 V bias voltage. (f) The gold surface bound AuNPs under influence of 0 V bias voltage.

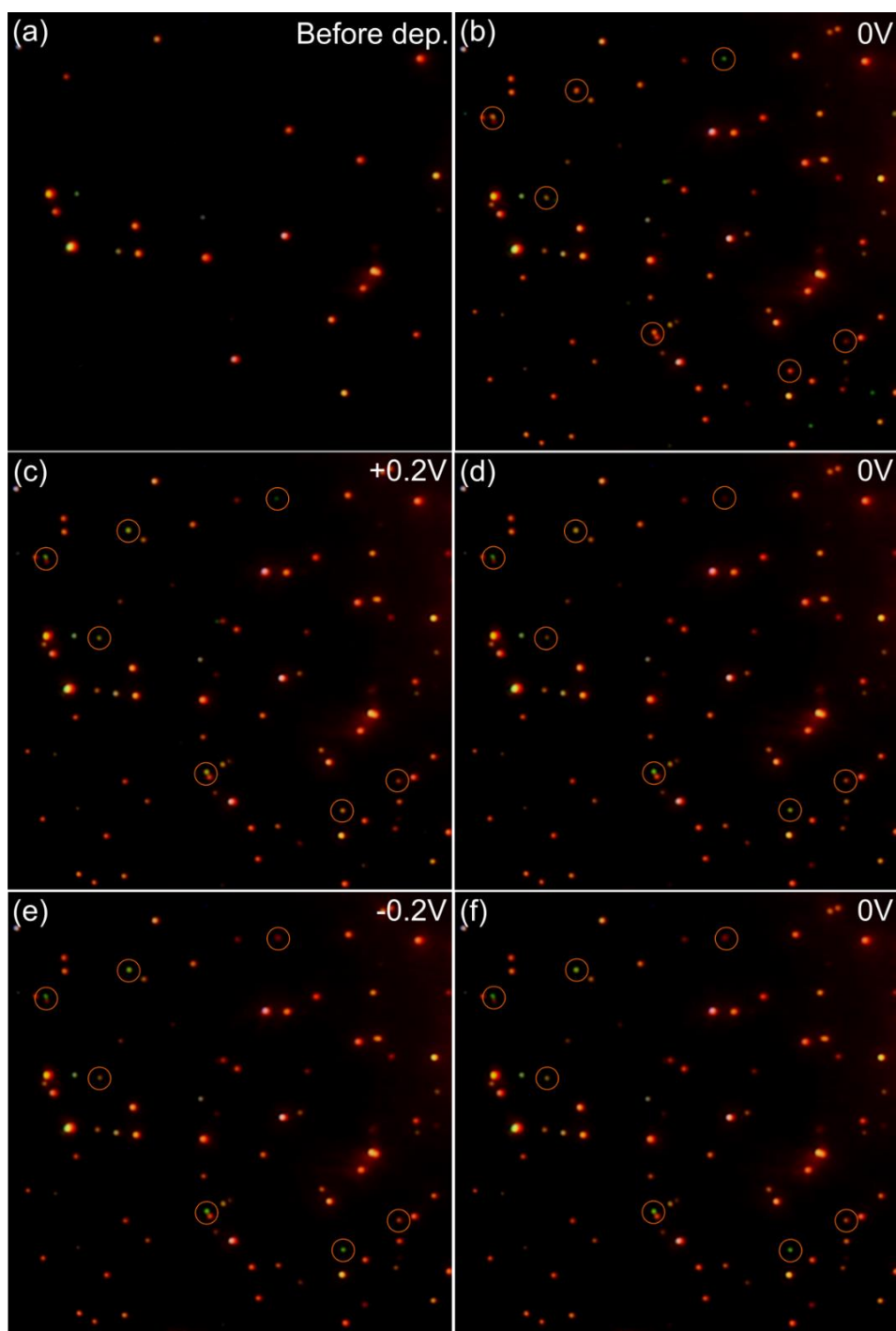


**Figure S8.** Additional dark field images of 0.1 % hairpin-DNA-AuNP sample before deposition and when the bias voltage was swept from 0 V to +0.2 V, then to -0.2 V and then back to 0 V. The AuNPs that change their color significantly during the measurements are circled. (a) The gold surface before AuNPs deposition. The objects seen in the image are surface defects. (b) The gold surface after AuNPs deposition and at zero biasing voltage. (c) The gold surface bound AuNPs under influence of +0.2 V bias voltage. (d) The gold surface bound AuNPs under influence of 0 V bias voltage. (e) The gold surface bound AuNPs under influence of -0.2 V bias voltage. (f) The gold surface bound AuNPs under influence of 0 V bias voltage.

## Note 7 - Calculation of electric field between the gold surface and ITO glass

In this work, we assumed that in the middle of the chip, where the measurements were carried out, the electric field was uniform. To estimate the electric field strength for DC-voltage in this region, we calculated the distance between the gold surface on silicon chip and the ITO glass above it. This was done by measuring the capacitance  $C$  between the plates and calculating the distance  $d$  using the plate capacitor equation

$$C = \frac{\epsilon_0 \epsilon_r A}{d}, \quad (1)$$

where the  $\epsilon_r$  is the relative permittivity of air, the  $\epsilon_0$  is the absolute permittivity and  $A$  is the area of the smaller surface. The applicability of equation 1 can be justified by two assumptions. First, the distance between the plates is much smaller than the size of the plates, which is valid, since the distance should be well under 1 mm and the size of silicon chip is 5.7 mm x 7.1 mm and the size of the ITO is 18 mm x 18 mm. Secondly, one of the plates is much larger than the other one, so that the edge effects can be ignored, which is valid since the ITO is considerable larger than the silicon chip. These assumptions mean that the smaller surface (gold surface) sees the larger surface (ITO) as a mirror surface with the same area as the gold surface and twice the distance  $d$  from the real, smaller surface. Since the electrostatic energy of this mirror system is twice that of the original system, then the capacitance is half of the original system. Now for the mirror system, the equation 1 is valid, and since we have twice the distance and half the capacitance and the capacitance of the original system simplify also into the equation 1.

The capacitance was measured using Wayne Kerr Automatic LCR Meter 4225, where  $C$  was 4.1 pF. By inserting the area of the silicon chip, the measured capacitance  $C$  and both permittivities into the equation 1, the distance  $d$  of 87  $\mu\text{m}$  was obtained. For biasing voltage of 1 V, the electric field strength corresponds to  $1.15 \cdot 10^4$  V/m.

## Note 8 - Hue versus LSPR scattering wavelength calibration

The Hue values are correlated to real colors as following<sup>3,4</sup> red is at 0°, green is at 120° and blue is at 240°. However, the Hue values related to the LSPR wavelengths of the gold particles are not well defined, so we measured LSPR scattering spectra of several particles and also took the corresponding optical images, and calculated the Hue value for each particle spectrum. This was done, because the LSPR peak can be related to the particle distance from the surface. The data was gathered from several samples, and, during the LSPR scattering measurements, the LSPR peak was tracked 1-2 min to ensure that particle was not moving and the color stayed unaltered.

The Hue values were calculated from RGB values by first solving the M, m and C parameters from equations below. Then these values combined with RGB values were used to calculate the corresponding H values. We used Matlab 2013a (version 8.1.0.604) for the numerical calculations. Figure S5 shows the Hue versus LSPR wavelength maxima plot. The H values roughly correspond to the theoretical values mentioned in the beginning of this section, since 0° is above 600 nm (red) and 120° is close to the 550 nm (green-yellow). The curve saturated after 610 nm, which is most probably due to fact that camera saturated to color RED. Also, the Hue is plotted in a circular scale with discontinuity around 0°, but the Hue values from zero to -50° are still associated to color red. Due of the camera saturation and the discontinuous circular scale, we related the Hue values below zero to wavelength of 610 nm or above. When combining the simulated LSPR scattering data from Figure 3 and the Hue versus LSPR maxima curve, it can be concluded that the H values close to 0°- 20° are associated to cases where particle is close to surface and particles with H value over 60° were found to be far away from the surface. This would roughly mean that 40° shift in H value is required to shift particle far away from the surface to close to the surface or vice versa.

$$\begin{cases} M = \max(R, G, B) \\ m = \min(R, G, B) \\ C = M - m \end{cases},$$
$$H = \begin{cases} 60^\circ \cdot \left( \frac{G - B}{C} \bmod 6 \right), & \text{if } M = R \\ 60^\circ \cdot \left( \frac{B - R}{C} + 2 \right), & \text{if } M = G \\ 60^\circ \cdot \left( \frac{R - G}{C} + 4 \right), & \text{if } M = B \\ \text{undefined}, C = 0, & \text{if } C = 0 \end{cases}$$

---

<sup>3</sup>Math behind colorspace conversion, RGB-HSL, <http://www.niwa.nu/2013/05/math-behind-colorspace-conversions-rgb-hsl/>

<sup>4</sup> Agoston, M.K. Computer graphics and Geometric Modelling v.1: Implementation and Algorithms, Springer, 301-304, 2004.

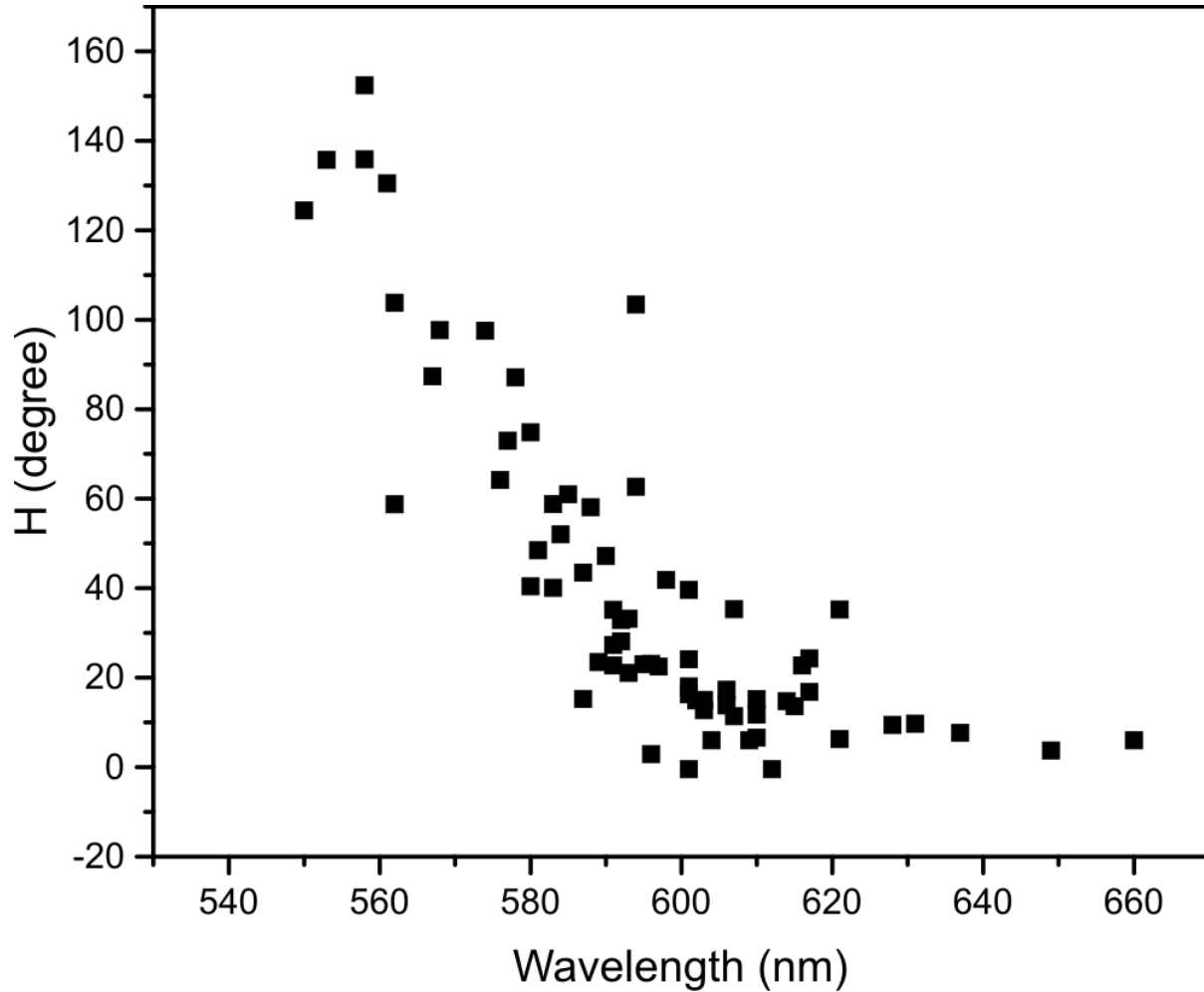


**Figure S9.** The calibration curve to correlate the LSPR wavelength of the AuNP to the corresponding Hue (H) values. When the particle is close to the gold surface ( $\lambda = 600 - 620$  nm or  $d = 3 - 5$  nm), the corresponding H values are  $0 - 20^\circ$ , and when the particle is far away from the gold surface ( $\lambda = 580$  nm or  $d = 12$  nm), the corresponding H values are above  $60^\circ$ .

## Note 9 - Histogram data of 8 nm and 3 nm ssDNA samples and overall histogram data

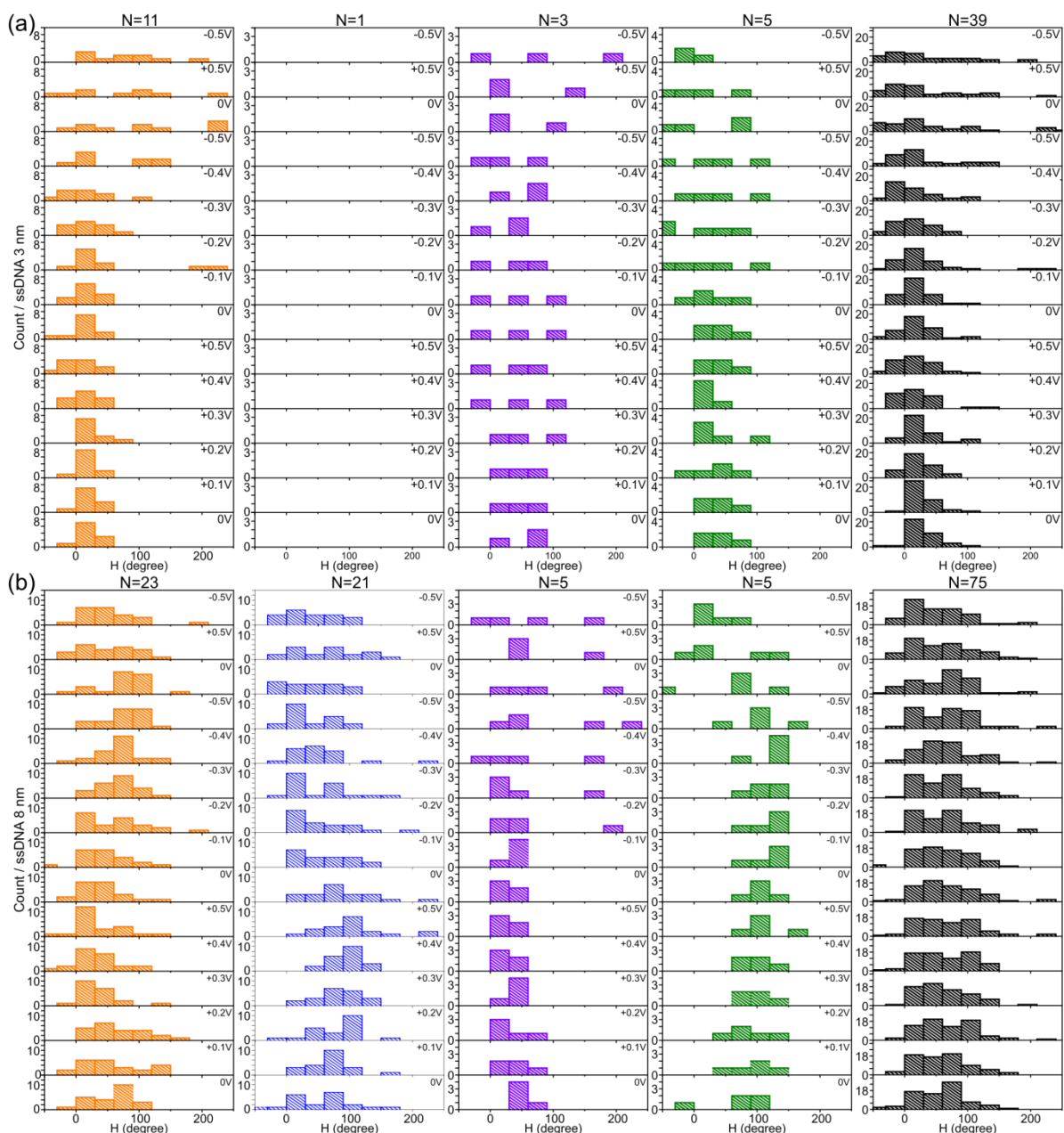


**Figure S10.** The histogram data of the (a) 3 nm DNA spacer samples functionalized with the ratio 0.1% and (b) 8 nm DNA spacer samples with the same ratio of the biotinylated spacer DNA. The orange histogram shows particles that move away from the surface with negative field. The blue histogram represent group of particles that behave opposite to particles in the orange histogram. The violet histogram shows particles that slowly move away from the surface and the green histograms shows particles that are stuck close to the surface. The black histogram shows data of all of the analyzed particles.

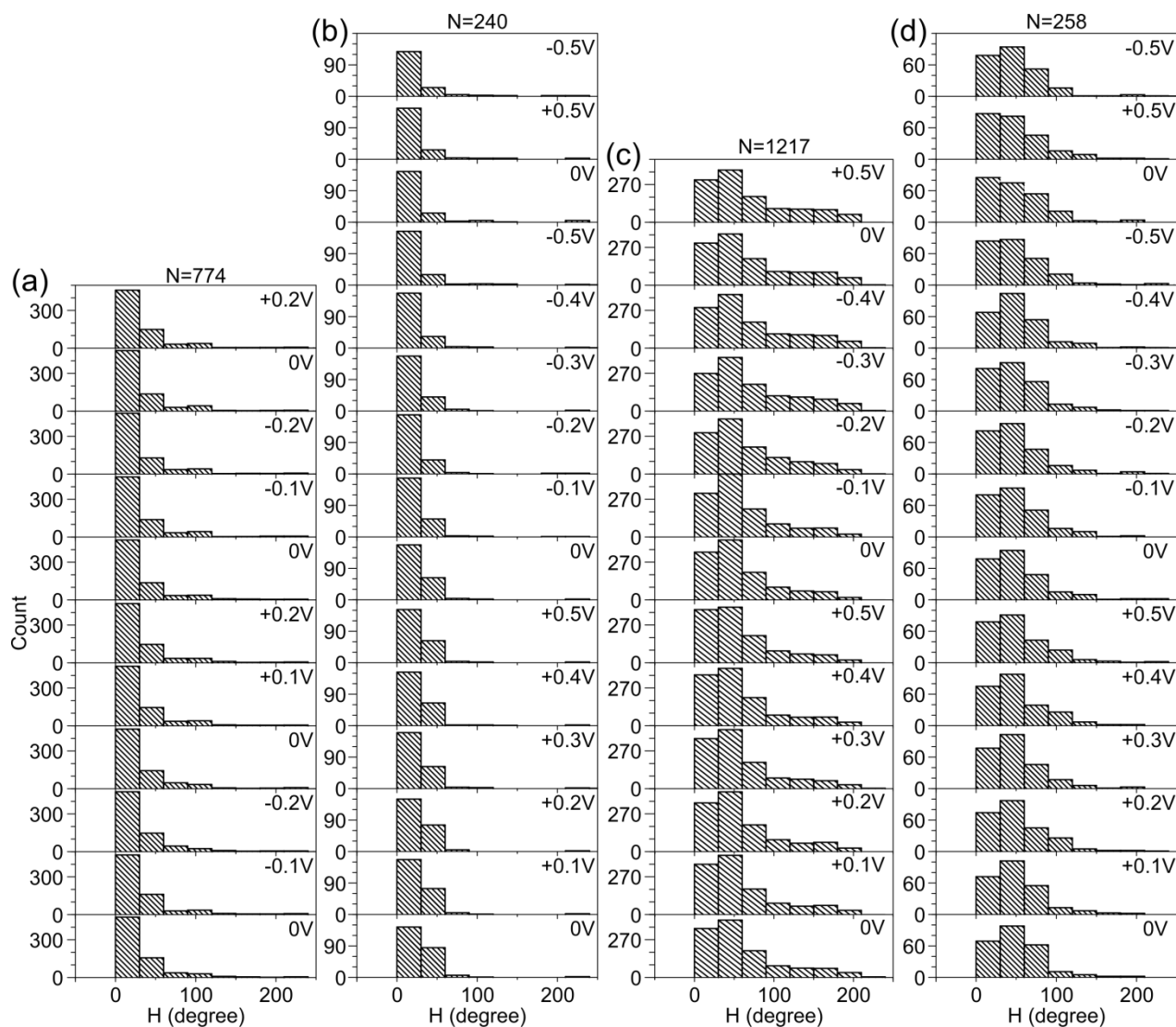


**Figure S11.** The overall histogram data of the AuNPs bound on gold surface. The numbers above the histograms indicate the number of analyzed particles. (a) Hairpin-DNA-AuNP sample shown in Figure 3a. (b) 3 nm DNA spacer sample shown in Figure S6a. (c) 15 nm DNA spacer sample shown in Figure 3b. (d) 10 nm DNA spacer samples shown in Figure S6b. The data shows that most of the particles are located near the gold surface during the measurements.

## Note 10 – Test with reduced amount of avidin and/or biotin

Here, our aim was to reduce the avidin density so that the particles would, on average, be bound to only one chimeric avidin and thus be more movable. Since the particle diameter was 80 nm, we adjusted the deposition time of the chimeric avidin to have roughly one avidin per 80 nm x 80 nm area. The usual deposition time was 30 min, while now we used 2 min, 1 min and 30 s to achieve lower densities. Figures S12b and s12e below show a sample with 1 min deposition time, where the avidin density is about 1.96 avidin per 80 nm x 80 nm area. Figures S12c and S12f show sample with 30 s deposition time, with chimeric avidin density of 1.12 avidin per 80 nm x 80 nm area. Both of these deposition parameters were further tested. Figure 1a shows result of 2 min deposition time, with a higher avidin density, and figure S12d shows a plain gold surface.

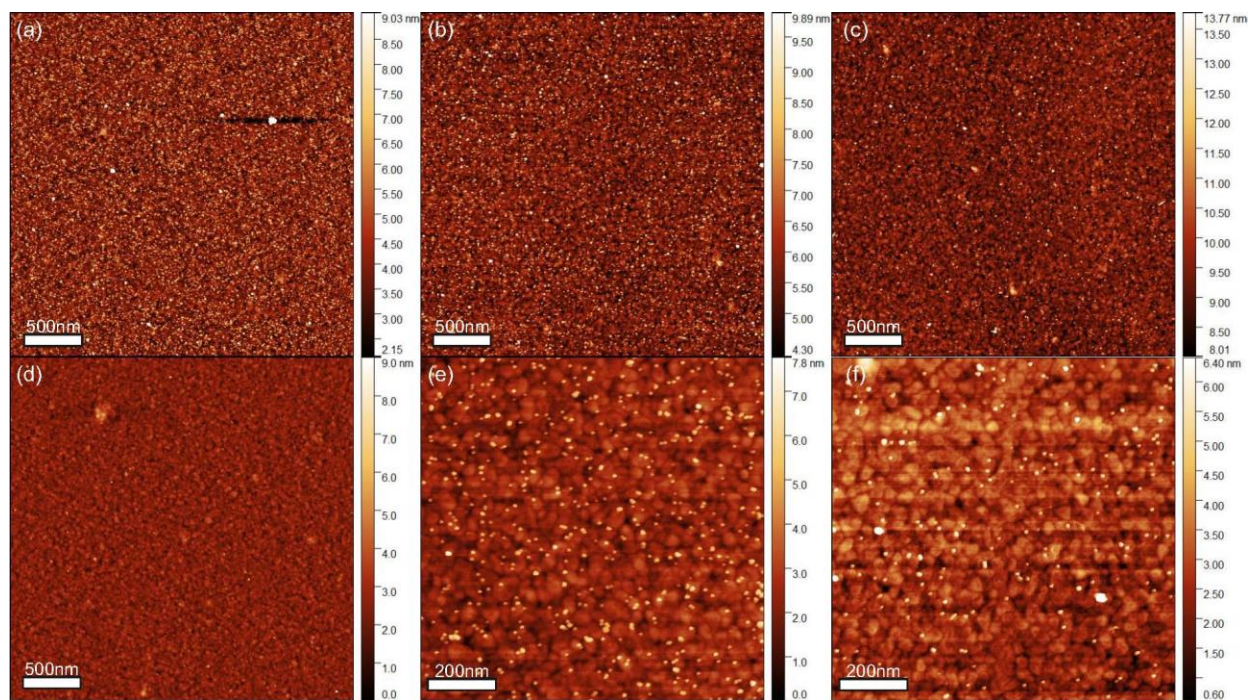


**Figure S12.** AFM images of (a) Gold surface after 2 min chimeric avidin incubation, (b) Gold surface after 1 min chimeric avidin incubation, and (c) Gold surface after 30 s chimeric avidin incubation. (d) A plain gold surface. (e) Close-up image of gold surface in figure b. The surface density of avidin is 1.96 per 80 nm x 80 nm area. (f) Close-up image of gold surface in figure c. The surface density of avidin is 1.12 per 80 nm x 80 nm area.

We used the 0.1 % hairpin-AuNPs and otherwise the same sample preparation. In the case of lowest avidin density (30 s deposition), almost no movement was observed while altering the electric field, and we could not divide the particles into separate groups. In some degree, the particle behavior followed that of the group 1 although not at all as clearly as in the Figs. 4. and S10. Notably was that, the overall particle distance from the surface was peaked at 50° in Hue-

scale, which is higher than for other samples. This means that the particles are overall bit further away from the surface. This would suggest that the particles are not as tightly bound to the surface as in the manuscript or that they are bound via non-specific bonding. The latter is more likely, since the non-specific binding also explains the lack of motion.

The Figure S13 shows the histogram data of all the movable particles as in the article for the sample with 1 min avidin deposition time. In this case the division into groups 1 to 4 was more evident, although the behavior of the particles is less prominent than in the article. Also, the percentages of particles in groups 1 and 2 are 5.2 % and 1.6 %, respectively, which is lower than for the regular samples. In general, the analyzed particles are located again further away from the surface ( $H = 50^\circ$ ) as shown in Figure S14 with histogram of all the analyzed particles on the sample.

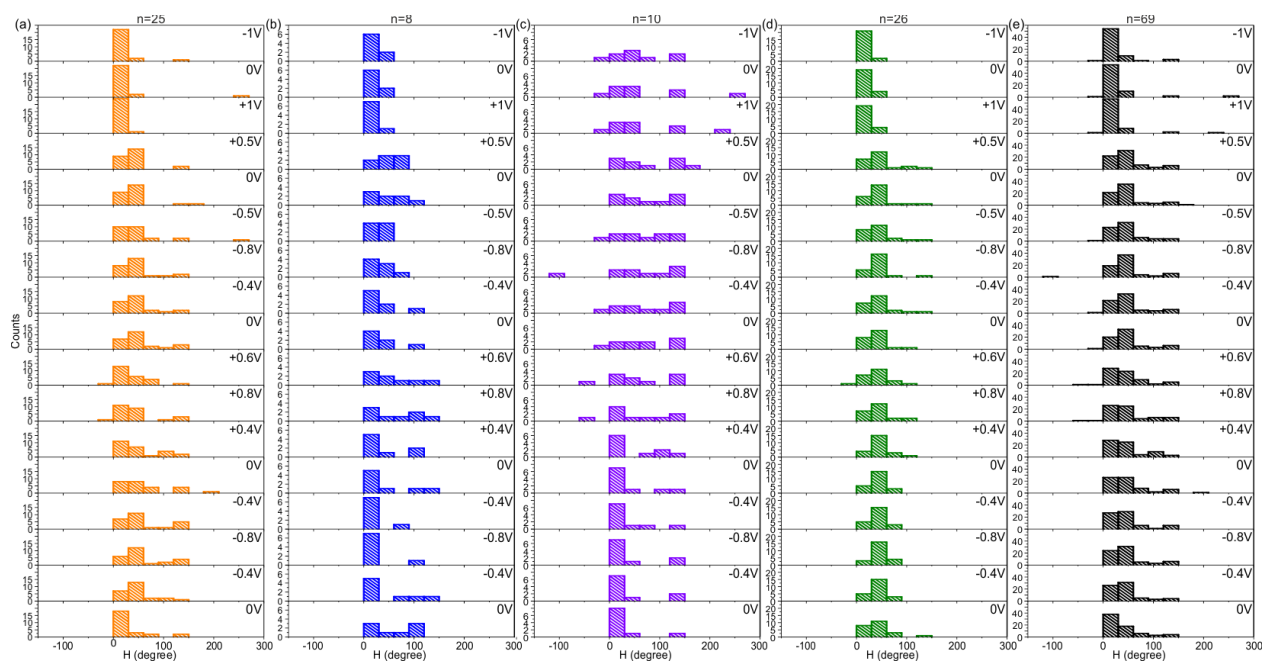


**Figure S13.** The histogram data of all color changing AuNPs conjugated with 0.1% of biotinylated hairpin-DNA (among the passivating DNA) bound to a surface with the surface density of chimeric avidin of 1.96 avidins per 80 nm x 80 nm area. The surface density of chimeric avidin is 1.96 avidin per 80nm x 80nm area. The numbers, n, above the histograms indicate the number of analyzed particles. (a) The orange histograms show particles that move away from the surface with negative electric field. (b) The blue histograms represent a group of particles that behave opposite to particles in the orange histograms. (b) The violet histograms show particles that slowly move away from the surface and the green histograms show particles that are stuck close to the surface. (d) The black histograms show data of all of the analyzed particles.

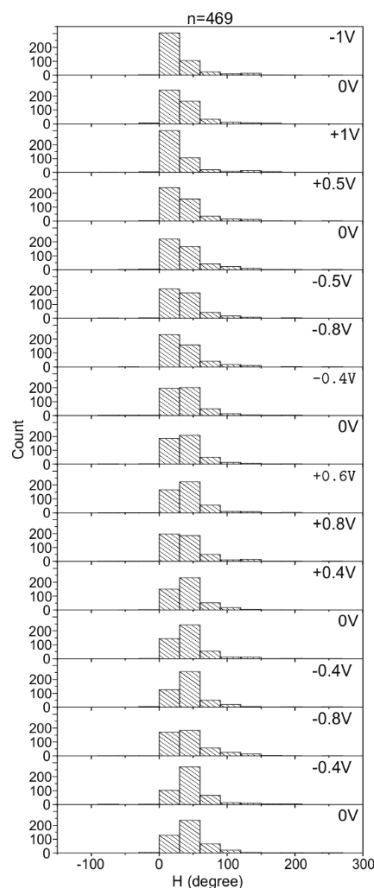


**Figure S14.** Histogram data of all the AuNPs bound on gold surface with the surface density of chimeric avidin of 1.96 avidins per 80 nm x 80 nm area. The number above the histogram indicates the number of analyzed particles.

We also fabricated AuNPs with lower hairpin-DNA density, i.e. with only 0.01 % hairpin-DNA portion, and immobilized them to a similar avidin coated surface as in the manuscript as well as to the surface with the reduced amount of avidin explained above (30 s deposition). As discussed, this would correspond to roughly 2 hairpin-DNA per nanoparticle. In this case the deposition time of AuNP was increased to 2.5 h, to allow binding even with reduced binding efficiency. However, this resulted in no discernible particle motion similarly to lowest amount of avidin coverage.

## Note 11 - More LSPR scattering spectra of hairpin-DNA-AuNPs

Figures S15a-d and S16a show the LSPR scattering spectra of pure hairpin-DNA-AuNPs, and Figure S16b shows the spectra of 0.1 % hairpin-DNA-AuNPs. The pure hairpin-DNA samples needed higher positive and negative voltages to move the particle compared to the 0.1% hairpin-DNA samples. In the case of Figure S15a, the LSPR peak has two equal peaks at 555 nm and 660 nm, when the particle is pulled toward surface using positive voltage, which corresponds to particle-surface distance  $d$  of 1-2 nm. When pushed away, there exists only one peak at 580 nm ( $d = 12$  nm). Similarly for the particle in Figure S15c, the LSPR peak has two equal peaks at 540 nm and 675 nm, when the particle is pulled toward surface using positive voltage, which corresponds to particle to the distance  $d$  of 1-2 nm. When pushed away, there exists only one peak at 570 nm ( $d = 20$  nm). The particle in Figure S15b has a double peak (585 nm and 670 nm) when pushed with negative voltage and single peak at 650 nm (1-2 nm) when pulled with positive voltage. The reason for double peaks is unknown, but ,as in the case of particle A and particle B, the particle in Figure S15b might experience fluctuation motion on and off the surface, where double peak consists of faraway (12 nm) and close proximity (1-2 nm) LSPR contributions. The particle in Figures 15d has one peak at 640 nm (3 nm) with negative voltage and one main peak at 680 nm and one small hump at 535 nm (orange line,  $d=1$  nm) with positive voltage, where the small hump is close to the secondary peaks observed in the simulations. Particle S16a behaves similarly as the particle C in Figure 5c. The particle in Figure S16b has only slight shift from 595 nm to 606 nm, when the voltage is altered from -0.4 V to +0.5 V and back to -0.4 V (the three top most bolded lines), which means shift from 7 nm to 4.5 nm and back to 7 nm.

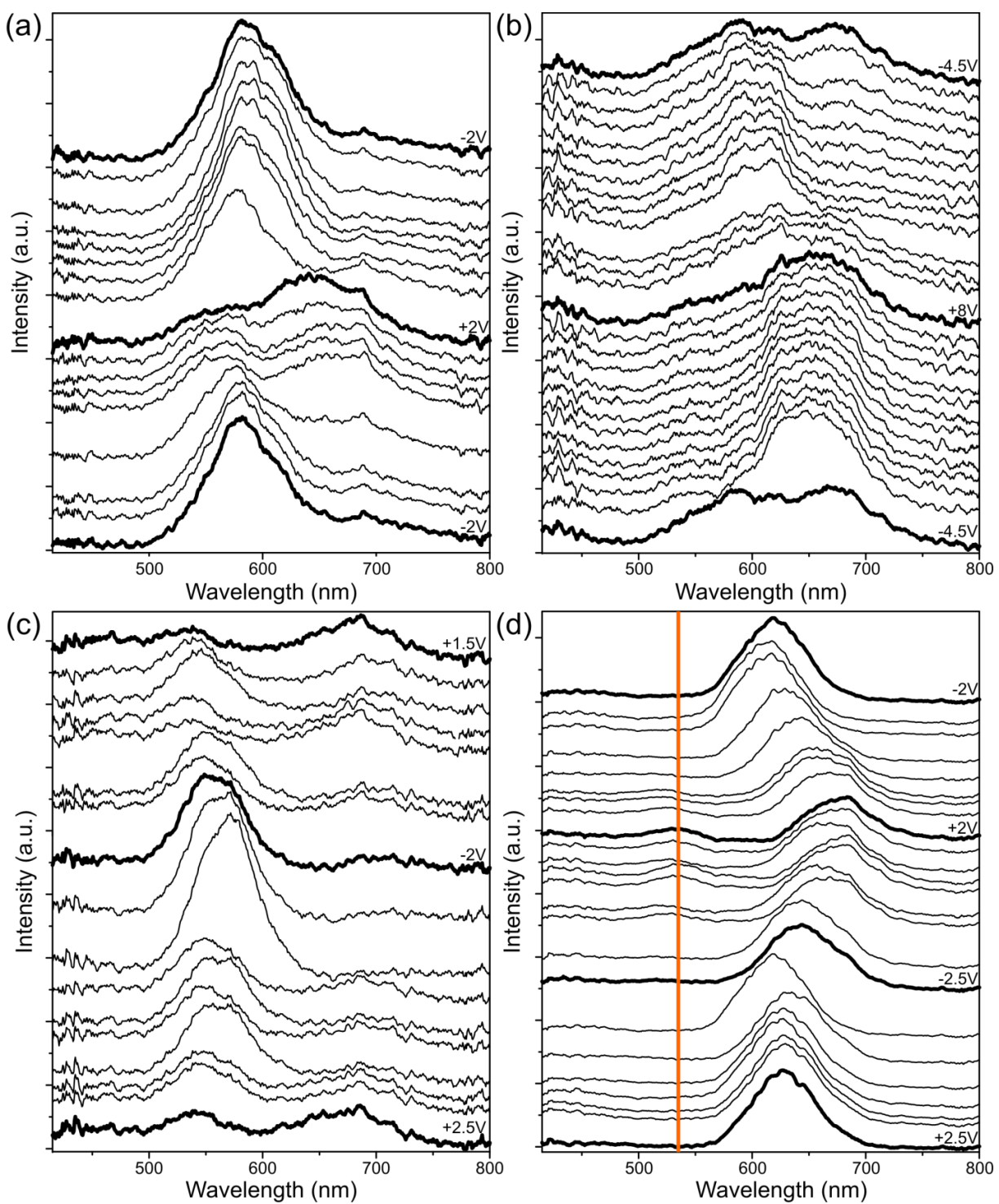


**Figure S15.** (a)-(d) Additional LSPR scattering spectra for pure hairpin-DNA-AuNP under influence of electric field. The particles in (a) and (c) have a double peak, when pulled with positive, and single main peak, when pushed with negative voltage. The particle in (d) has a single main peak, when pushed with negative and pulled with positive voltage, and a small hump at 535 nm indicated by orange line, when pulled with positive voltage. The particle in (b) has a double peak with negative voltage and a single peak with positive field.

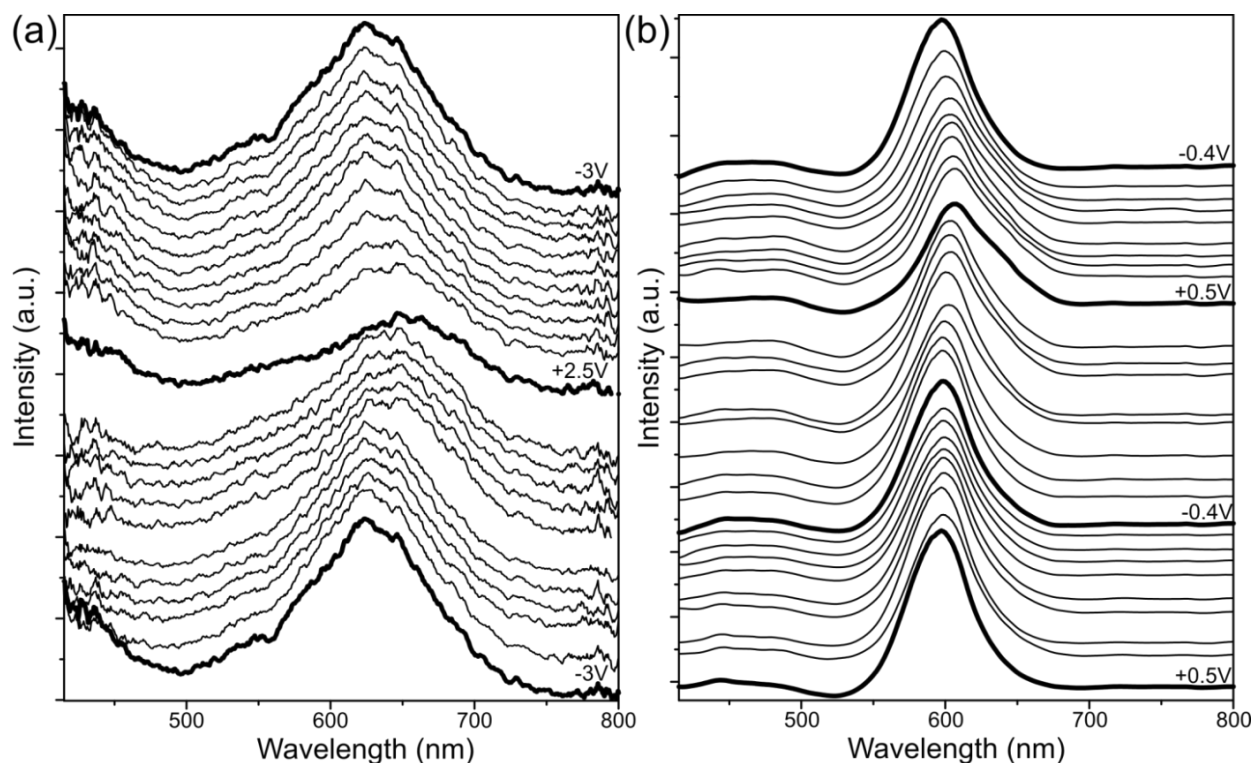


**Figure S16.** Additional LSPR scattering spectra of hairpin-DNA-AuNPs under influence of electric field. (a) The LSPR scattering spectra of pure hairpin-DNA-AuNP. (b) The LSPR scattering spectra of 0.1% hairpin-DNA-AuNP.

## Note 12 - Numerical simulations

The plasmonic properties of the gold nanoparticle and gold surface were characterized using the finite element method (FEM). We used RF module of the Comsol Multiphysics 5.1 modeling software in all of the numerical calculations to solve the scattering cross section of a 80 nm diameter gold nanoparticle as a function of distance  $d$  between the surface and the particle. The Scatterer on substrate<sup>5</sup> application in Comsol was used as a template, where we replaced the original scatterer model with 80 nm sphere and modified the surface and the nanoparticle to incorporate the complex refractive index of gold from Johnson and Christy<sup>6</sup>. Also, the angle scanning was turned off and we used fixed the incident angle of excitation light of  $70^\circ$  in respect to the axis normal to the Au-surface, which correspond to the incident angle for the 50x Olympus dark field objective. Since we used non-polarized light, both TE and TM polarized light are considered in the simulations. For simplicity, we assumed homogeneous water medium ( $n = 1.33$ ) surrounding the particle and on the surface of the particle, which is fairly reasonable assumption, since the LSPR peak of the AuNP after DNA functionalization did not shift

<sup>5</sup> Comsol application ID:14699

<sup>6</sup> Johnson, P.B; Christy, R.W. Optical Constants of the Nobel Metals. *Phys.Rev.B* **1972**,6, 4370-4379.

significantly from the original peak position. For both polarization, the distance  $d$  was changed from 20 nm to 1 nm, and for each simulated distance the wavelength of the incident light was scanned from 480 nm to 750 nm as shown in Figure 3. We also plotted the field enhancement for different AuNP-Au-surface configuration as shown in Figures 3 and S17. Figures S17a and S17b show the field enhancement of AuNP for TM and TE polarizations respectively, when the distance  $d$  is 20 nm, and Figures S17c and S17d show the field enhancement of AuNP for TE polarization at 545 nm and 615 nm excitations respectively, when the distance  $d$  is 3 nm.

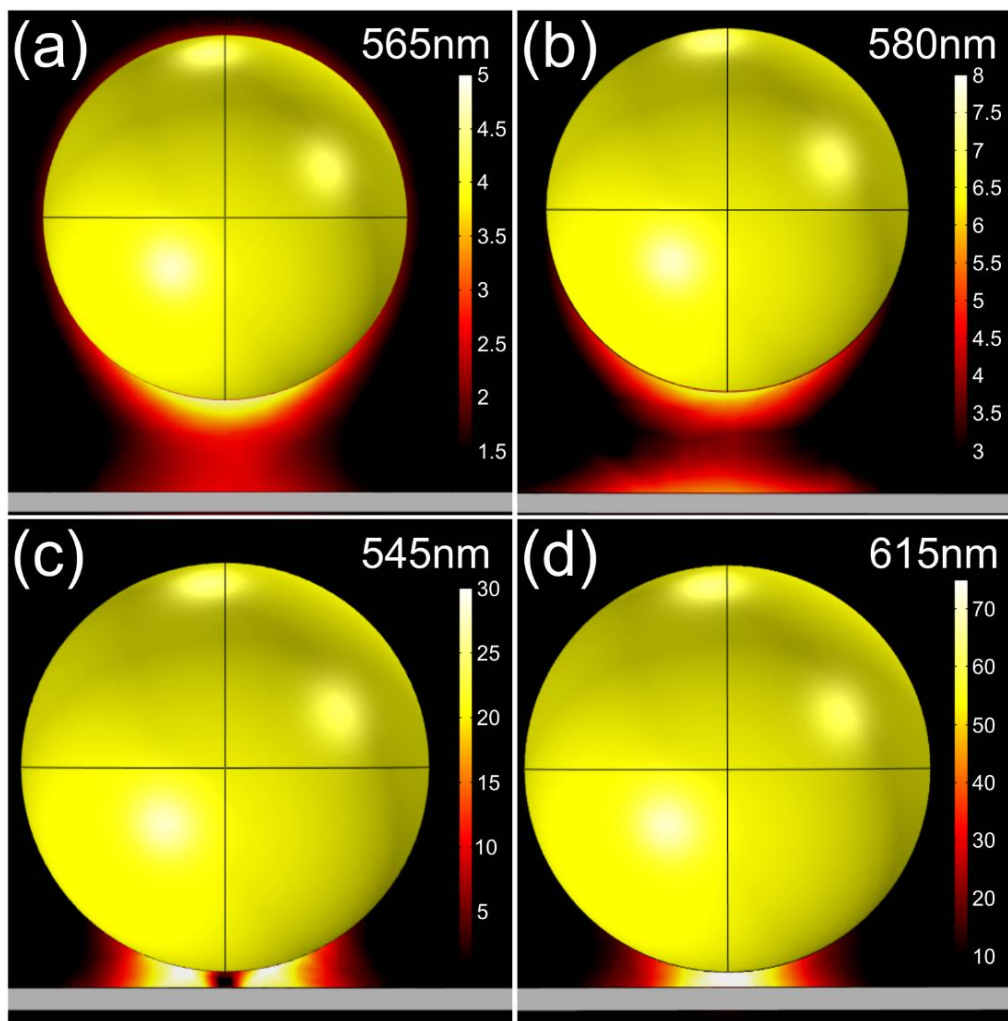


**Figure S17.** Additional field enhancement images of 80nm AuNP near the gold substrate. (a) The field enhancement of the AuNP-Au-substrate system for TM polarization, when the excitation wavelength is 565 nm and the distance  $d$  is 20 nm. (b) The field enhancement of the AuNP-Au-substrate system for TE polarization, when the excitation wavelength is 580 nm and the distance  $d$  is 20 nm. (c) The field enhancement of the AuNP-Au-substrate system for TE polarization, when the excitation wavelength is 545 nm and the distance  $d$  is 3 nm. (d) The field enhancement of the AuNP-Au-substrate system for TE polarization, when the excitation wavelength is 615 nm and the distance  $d$  is 3 nm.

## Note 13 - DNA strands

**Table S3:** The DNA strand used in the nanoactuator study.

Strand	DNA sequence
hairpin-DNA	/5BiosG/AAAAAAAAAAAAAAAAAATACCCGGGCGTTTTTCGCCCGGTAAAAAAAAA/3ThioMC3-D
DNA-s15nm	/5BiosG/ACA/3ThioMC3-D/
DNA-s8nm	/5BiosG/ACACACACACACACACACACACACAC/3ThioMC3-D/
DNA-s3nm	/5BiosG/ACACACACAC/3ThioMC3-D/